Title of Grant: "Experimental Studies of High-Energy Processing of Proto-Planetary and Planetary Materials in the Early Solar System"

Annual Report to DOE-NNSA – Year3

PI: Stein B. Jacobsen Period: 03/01/08 - 02/28/09

Name and Address of Recipient Institution: Harvard University, 1350 Massachusetts Avenue, Suite 727, Cambridge, MA 02138

Grant number: DE-FG52-06NA26215

MANAGEMENT REPORTING Progress Report

1. The DOE award number and name of the recipient.

DE-FG52-06NA26215, Harvard University.

2. The project title and name of the project director/principal investigator.

Project Title: Experimental Studies of High-Energy Processing of Proto-Planetary Materials in the Early Solar System
Principal Investigator: Stein B. Jacobsen

3. Date of report and period covered by the report.

3/1/2008—2/28/2009

4. A comparison of the actual accomplishments with the goals and objectives established for the period and reasons why the established goals were not met.

Year 3 Goals and Objectives: Finishing up experimental studies of metal-silicate miscibility at different P and T; writing up the final results. Pilot study of chondrule formation: configuration of the laser for IR and green radiation; irradiation of chondrule targets by the IR and green radiation and analyses of evaporation and ablation processes; thorough characterization of the experimental charges; testing of chondrule formation models.

The third year goals and objectives were met. The experiments on metal-silicate mixtures have been completed. We were and still are working on publications of the results in major journals such as Nature and Earth and Planetary Science Letters. The pilot study on chondrule formation showed that very high energy density in our experiments, although capable of melting solid silicate-metal mixtures, results in almost instantaneous removal of the melt from the surface rather then in melting of a whole object, contrary to the chondrule properties. Further experiments on this topic were found to be counterproductive.

5. A discussion of what was accomplished under these goals during this reporting period, including major activities, significant results, major findings or conclusions, key outcomes or other achievements. This section should not contain any proprietary data or other information not subject to public release. If such information is important to reporting progress, do not include the information, but include a note in the report advising the reader to contact the Principal Investigator or the Project Director for further information.

Analytical work was focused on identification of the source of Cr and Al in the shock-produced melts. A detailed analysis of the chemical data on the shock melts and minerals of the ALM dunite showed that both Cr and Al are supplied by minute grains of chlorite, with contributions from other minerals being negligible. This finding, in turn, led to the development and calibration of the model for scaling of the Richmyer-Meshkov mixing from our experiments to planetary and astrophysical environments.

Theoretical part of the study was aimed at the development and calibration of a scaling model for the Richtmyer-Meshkov instabilities. We found that the RM instability scale (L) for a shock wave driven process in dense (molten) liquids is obtained from the following simple relationship: $L = -2An\tau U_T \ln x$, where $A = \sim 0.4$ is the Atwood number, τ is the shock pulse time, UT - the isothermal speed of sound in the plasma, and $x = m(t)/m_o$, m(t) is the remaining mass at time t, and m_o is the initial mass. Because L is based on the so-called "Euler similarity" and the Euler's equations remain scale invariant from μm-mm scale laser experiments to large-scale astrophysical phenomena such as supernova explosions, our scaling equation is valid for all aspects of hydrodynamic instabilities including the Richmyer-Meshkov, Rayleigh-Taylor, and, likely, Kelvin-Helmholtz instabilities.
The application of our experimental results to the problem of chondrule formation shows that very high energy density in our experiments, although capable of melting solid silicate-metal mixtures, results in almost instantaneous removal of the melt from the surface rather then in melting of a whole object, contrary to the chondrule properties. Further experiments on this topic were found to be counterproductive.

6. Cost Status. Show approved budget by budget period and actual costs incurred. If cost sharing is required break out by DOE share, recipient share, and total costs.

Cost status was submitted by Office of Sponsored Programs (OSP) at Harvard in the form of the Financial Status Report.

7. Schedule Status. List milestones, anticipated completion dates and actual completion dates. If you submitted a project management plan with your application, you must use this plan to report schedule and budget variance. You may use your own project management system to provide this information.

Year 3 Schedule (same as goals and objectives): All relevant experiments have been completed. The results are reported at several conferences. Several papers are either submitted or being prepared for publication in major journals. The pilot study of chondrule formation showed that further experiments relevant to this subject are counterproductive.

We have completed all of the third-year milestones on time.

8. Any changes in approach or aims and reasons for change. Remember significant changes to the objectives and scope require prior approval by the contracting officer.

No

9. Actual or anticipated problems or delays and actions taken or planned to resolve them.

None

10. Any absence or changes of key personnel or changes in consortium/teaming arrangement. Include a table listing name, citizenship, and position of all personnel supported under the grant and note if students have graduated and if they accepted a position with a national lab.

No personnel changes

11. A description of any product produced or technology transfer activities accomplished during this reporting period, such as:

A. Publications (list journal name, volume, issue); conference papers; or other public releases of results.

J. L. Remo and M. D. Furnish, Analysis of Z-pinch shock wave experiments in meteorite and planetary materials, Intl. J. Impact Eng., 35, 1516-1521, 2008.

S. B. Jacobsen, M. C. Ranen, M. I. Petaev, J. L. Remo, R. J. O'Connell, and D. S. Sasselov, Isotopes as clues to the origin and earliest differentiation history of the Earth, Phil. Trans. R. Soc. A, 366, 4129–4162, 2008.

J. L. Remo and R. G. Adams, High energy density laser interaction with planetary and astrophysical materials: methodology and data, High-power laser ablation VII (ed. C. R. Phipps), Proc. SPIE, 7005, 70052m-1–70052m-10, 2008.

J. L. Remo, Plasma radiation hydrodynamics and momentum coupling, High-power laser ablation VII (ed. C. R. Phipps), Proc. SPIE, 7005, 70052j-1–70052j-9, 2008.

S. B. Jacobsen, J. L. Remo, M. I. Petaev, and D. S. Sasselov, Hf-W Equilibration in a Magma Ocean at Very High P and T, Geochim. Cosmochim. Acta, **72**, Supplement 1, A419.

S. B. Jacobsen, J. L. Remo, M. I. Petaev, and D. S. Sasselov, Hf-W chronometry and the timing of the giant Moon-forming impact on Earth. Lunar Planet. Sci. Conf, 40, 2054, 2009.

J. L. Remo, S. B. Jacobsen, M. I. Petaev, R. G. Adams, and D. D. Sasselov, Laser shock melting of a metal-silicate target and the timing of the giant Moon-forming impact on Earth, Nature, under revision, 2009.

S. B. Jacobsen, J. L. Remo, M. I. Petaev, and D. S. Sasselov, The first law of cosmochemistry, Geochim. Cosmochim. Acta, in press, 2009.

M. I. Petaev, S. B. Jacobsen, J. L. Remo, R. G. Adams, and D. S. Sasselov, Experimental study of high-energy processing of protoplanetary materials: implications for the post giant impact Earth, Earth Planet. Sci. Lett., in preparation, 2009.

B. Web site or other Internet sites that reflect the results of this project.

None

C. Networks or collaborations fostered.

Collaboration with Sandia National Laboratory

D. Technologies/Techniques.

A new technique for quantifying shock-induced mixing both in laser-ablation experiments and during the giant impact phase of planetary formation

E. Inventions/Patent Applications

None

F. Other products, such as data or databases, physical collections, audio or video, software or netware, models, educational aid or curricula, instruments or equipment.

None

FINAL REPORT to the DOE award:

DE-FG52-06NA26215

Recipient:

Harvard University, 1350 Massachusetts Avenue, Suite 727, Cambridge, MA 02138

Project Title:

Experimental Studies of High-Energy Processing of Proto-Planetary and Planetary Materials in the Early Solar System

Principal Investigator:

Prof. Stein B. Jacobsen, Department of Earth and Planetary Sciences, Harvard University (jacobsen@neodymium.harvard.edu)

Co-Investigators:

Prof. Dimitar Sasselov, Department of Astronomy, Harvard University (dsasselov@cfa.harvard.edu)

Dr. Michail I. Petaev (Staff Scientist), Department of Earth and Planetary Sciences, Harvard University (mpetaev@cfa.harvard.edu)

Dr. John L. Remo (Research Associate), Department of Earth and Planetary Sciences, Harvard University (jremo@cfa.harvard.edu)

1. Executive summary

The results of this project are the first experimental data on the behavior of metal-silicate mixtures under very high pressures and temperatures comparable to those of the putative Moon-forming impact experienced by Earth in its early history. Probably the most important outcome of this project was the discovery that metal-silicate interaction and equilibration during highly energetic transient events like impacts may be extremely fast and effective on relatively large scale that was not appreciated before. During the course of this project we have developed a technique for trapping supercritical melts produced in our experiments that allows studying chemical phenomena taking place on a nanosecond timescales. Our results shed new light on the processes and conditions existed in the early Earth history, a subject of perennial interest of the humankind. The results of this project also provide important experimental constraints essential for development of the strategy and technology to mitigate imminent asteroid hazard.

2. Project objectives and accomplishments

The major objective of the project was an experimental study of physical and chemical interaction between mantle (olivine) and core (metal) materials at very high temperatures (>4000 K) and pressures (>135 GPa) that are thought to have existed during and after the putative giant impact responsible for the formation of the Earth-Moon system. As a minor task, we proposed to carry out a pilot study of interaction of high energy radiation with mixed metal-silicate targets in order to evaluate a feasibility of this process for chondrule formation in putative radiation driven nebular shock waves.

To achieve these objectives we developed:

- an experimental setup for irradiating our targets with powerful SNL lasers
- a technique for preparation of powdered samples and fabrication of target pellets
- proper target holders capable of recovering of the irradiated samples
- mathematical models for proper calculations of the P-T conditions of our experiments based on a limited number of measurable characteristics
- mathematical models for scaling the experimental results to planetary and astrophysical environments.

The application of the above techniques to solid and powdered metal-silicate targets along with petrologic and chemical studies of the irradiated targets allowed:

- to measure shock parameters as particle velocity, shock velocity, pressure gradient, and the momentum coupling coefficients for a variety of materials
- to establish a range of laser irradiation parameters (laser intensity, pulse duration, spot size) optimal for producing high T-P melts while still retaining them within intact or partially broken targets
- to estimate with sufficient precision the peak pressures and temperatures of target melting
- to establish the ranges of chemical variations in the silicate and metallic melts coexisting at high pressures and temperatures of our experiments
- to justify the use of the Hf-W chronometer for dating core formation and early differentiation of terrestrial planets

The application of our experimental results to the problem of chondrule formation showed that very high energy density in our experiments, although capable of melting solid silicate-metal

mixtures, results in almost instantaneous removal of the melt from the surface rather then in melting of a whole object, contrary to the chondrule properties. Further experiments on this topic were found to be counterproductive.

3. Project activities

This extended summary describes the main accomplishments of the project such as (1) the experimental setup, (2) new experimental techniques developed for trapping the high T,P melt, (3) mineralogy and chemistry of the experimental charges, and (4) implications of our experimental results to the evolution of Earth-Moon system.

3.1 Development of the experimental setup

To evaluate the behavior of metal-silicate mixtures at giant impact conditions we carried out experiments aimed at studying partitioning of Fe and Ni (proxy for W) between metal and silicate melt formed at high P and T by laser-driven shocks of powdered ultra-pure Fe metal and Ni-bearing ALM-2 dunite mixtures.

The targets were fabricated by pressing (at ~40 kPsi) mixtures of the vapor-deposited Ni-free Fe metal crystals (20-50 μm) and powdered ALM-2 dunite (5-300 μm) into disk-shaped pellets of 6.3 mm in diameter and ~1-2 mm thick. The ALM-2 dunite (from Almklovdalen, Norway) consists of forsterite (Fo 93.1±0.5, NiO ~0.4 wt. %) with minute grains of clinopyroxene, orthopyroxene, Al-rich chlorite, and chromite (Fig. 1). Target porosities of 20-35 % were evaluated from the back-scattered electron (BSE) images.

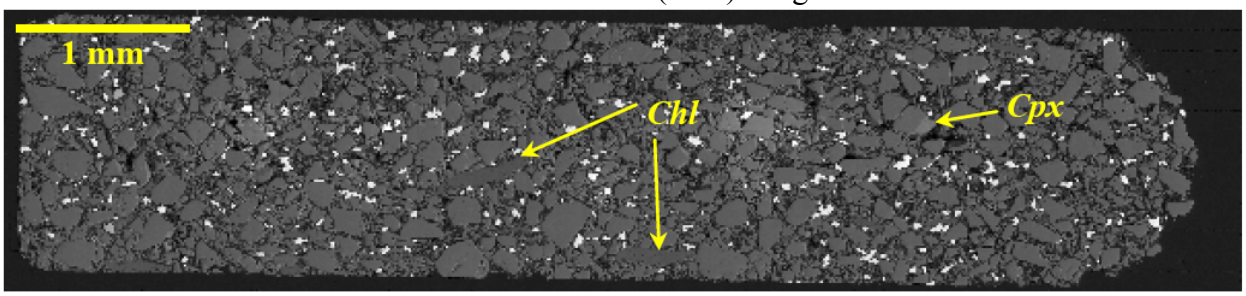

Figure 1. BSE image of the target (90 % dunite and 10 % metal). Black – epoxy, white – metal, gray – silicates, mainly forsterite. Minute grains of clinopyroxene (Cpx) and chlorite (Chl) are shown by labeled arrows.

The experiments on laser shock-induced melting of metal-dunite targets were conducted at the Sandia National Laboratories using NLS (1064 nm) and ZBL (527 nm) lasers with maximum energy outputs of 300 GW/cm^2 and ~10 TW/cm^2, respectively. Evidence of melts was only found in the targets irradiated with the ZBL laser.

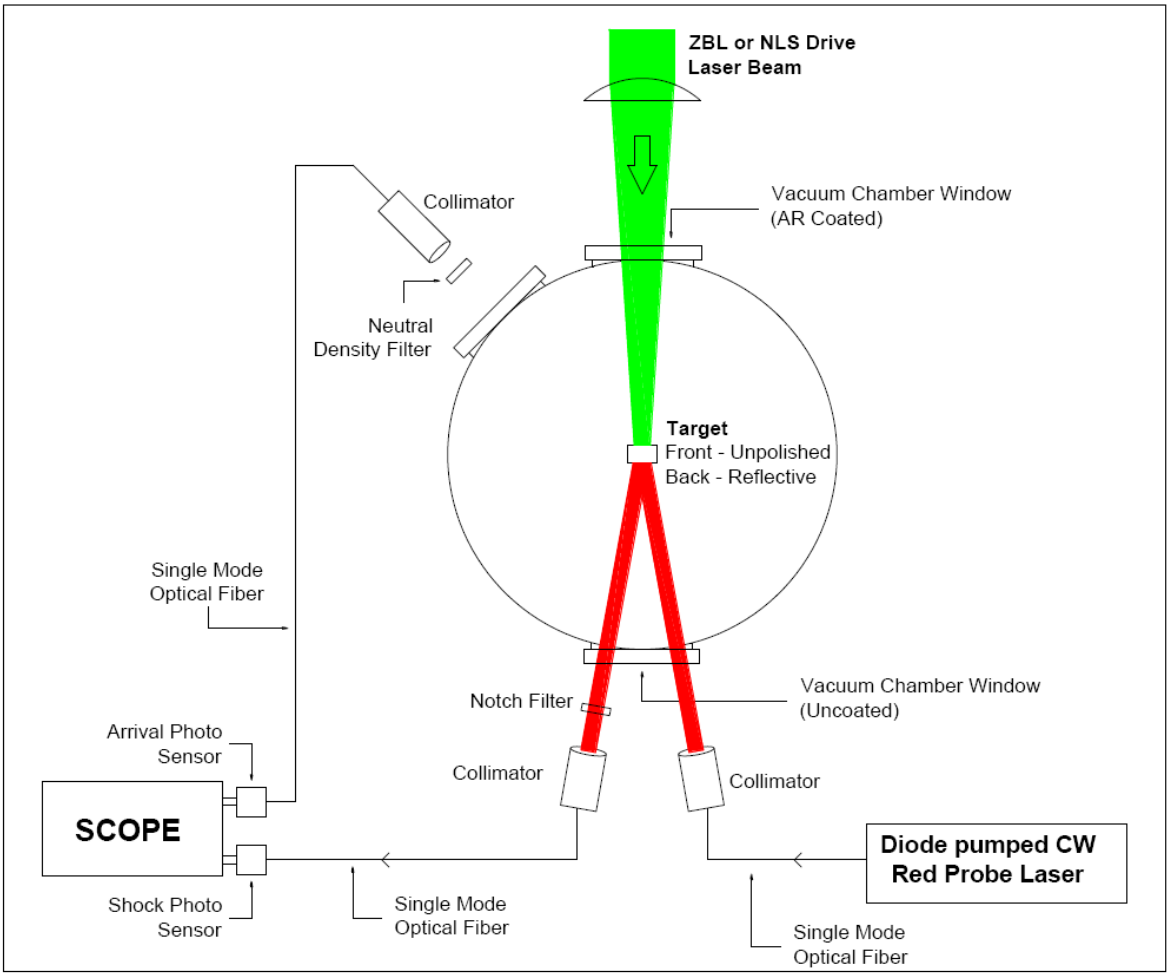

Figure 2. Schematic diagram of experimental setup.

The targets, one at a time, sealed in a vacuum chamber ($<10^{-4}$ torr) were shocked by a single pulse of either 1064 or 527 nm laser radiation focused to ~1 mm spot. The intensity of laser radiation for each experiment was calculated based on the measured energy output, pulse length, and spot size of a particular laser shot. The experimental setup (Fig. 2) allowed an automatic detection of the arrival of the shock wave, monitoring its propagation through the target, and precise measurement of the target rear surface displacement. Plasma radiation from the pulsed laser impact on the front surface is detected and initiates a time sequence. A probe laser signal monitoring the rear surface detects the emergence of the shock wave at the rear surface. The rear surface push-out time is measured from the shock wave arrival time to the time taken for the signal to reach its minimal value, indicating complete laser beam displacement from the rear surface probe detector. The real-time electro-optical recordings of the shock wave propagation and particle velocities coupled with the known irradiation intensity were used to calculate the shock parameters of each experiment (section 3.3).

3.2 Summary of experimental results

Shock-induced melts were only found in the targets (ZBL-10, -13, and -16) irradiated with the 527 nm ZBL laser, delivering ~140-400 J per 0.15-1 nsec pulse. At lower pulse energies no

melting was observed while at higher energies targets did not survive. The laser shot created a plasma cloud above the target surface and an ablation region of a high density melt at the plasma-target interface that eventually produced a "crater" (Fig. 3A,C).

Recovered targets or their fragments show more or less rounded craters with blackened appearance. BSE images of cratered target fragments (Fig. 3) show rough crater surfaces with host metal and forsterite grains being bound together by thin films or pockets of silicate melt with varying amounts of dispersed metal beads. No traces of melt were found on crater surfaces. Melt apparently fills porous space, grain boundaries, and cracks and crevasses in forsterite grains. No evidence for incipient melting such as reaction relationships among metal-silicate melt and host metal and forsterite grains was found in the targets studied, so far. Moreover, optical properties of forsterite grains surrounded by melt (*e.g.*, Fig. 3B) show no evidence of experiencing high temperatures and pressures.

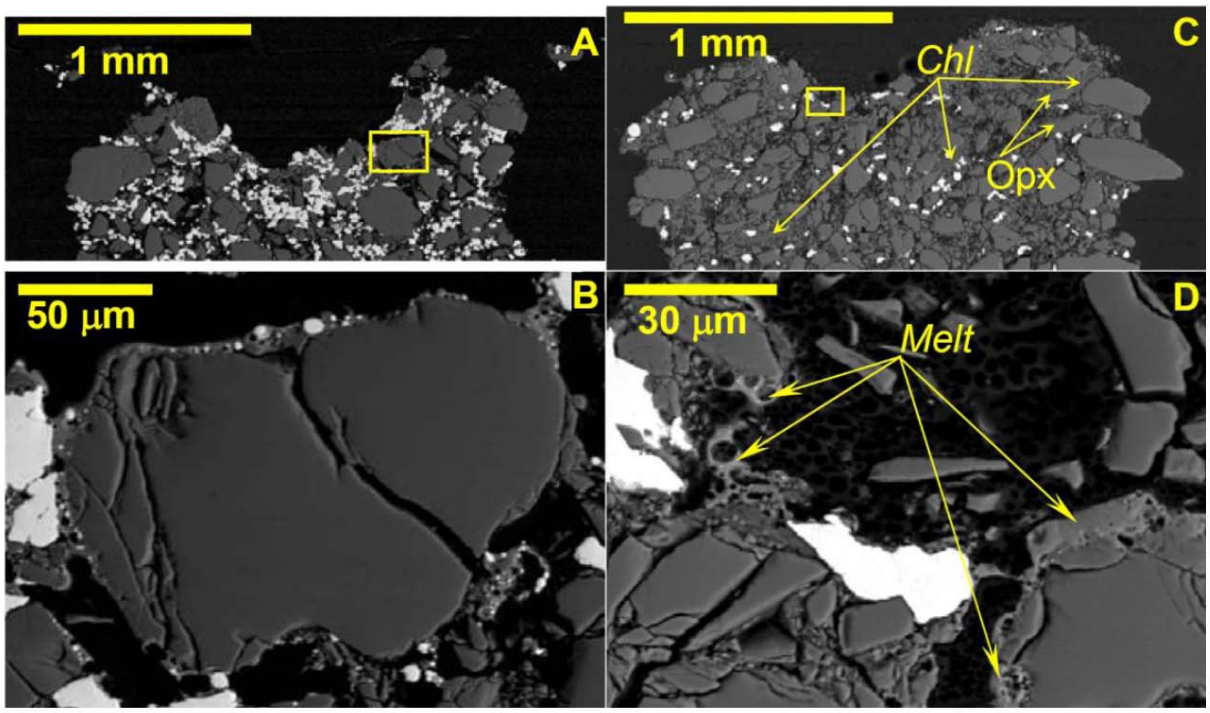

Figure 3. BSE images of the targets studied. Black – epoxy, white – metal, gray – silicates, mainly forsterite. Minute grains of chlorite (Chl), and orthopyroxene (Opx) are shown by labeled arrows. A: Cratered fragment of the target ZBL-16 (50 % dunite and 50 % metal) shocked at 276 GPa. The yellow box outlines area shown in B. B: Forsterite grain surrounded by a discontinuous rim of FeO-rich silicate melt (lighter gray) with embedded metal beads. Note the lack of reaction between the melt films and host forsterite and metal. C: Cratered fragment of the target ZBL-13 (90 % dunite and 10 % metal) shocked at 228 GPa. The yellow box outlines area shown in D. D: Pockets of FeO-rich silicate melt rimming forsterite grains in a cavity underneath the crater surface. The presence of vesicles in the melt points to some boiling after the pressure release.

Chemical compositions of silicate melt and metal beads differ significantly from the host olivine and metal, respectively (Fig. 4). Silicate melt is enriched in Al_2O_3, Cr_2O_3, and FeO compared to the host forsterite. NiO concentrations in silicate melt depend upon the presence or lack of metal beads in it: silicate melt without metal beads has NiO contents similar to that of the host forsterite, while silicate melt with abundant metal beads is depleted in NiO. Simultaneously, metal beads contain substantial amounts of Ni and Si, providing direct evidence for the extraction of Ni and Si from the silicate melt into the coexisting metal. The generally small sizes

of metal beads, typically in the 3-5 micrometer range, imply that their analyses might have been contaminated with the surrounding silicate melt due to the beam overlap. In many cases this can be verified by the rather high Si (a few wt. %) contents in metal beads; such analyses are not reported here. To test whether the low Si contents in metal are real, we measured a compositional profile across one large metal bead shown in Fig. 4E. The rather high Si contents in the core of this bead suggest that the Si concentrations measured in other beads are real and not a result of X-ray fluorescence from the surrounding silicate melt. Moreover, the pronounced Si zoning points to a diffusional loss of Si from the metal upon cooling that, however, apparently did not affect the Ni concentration.

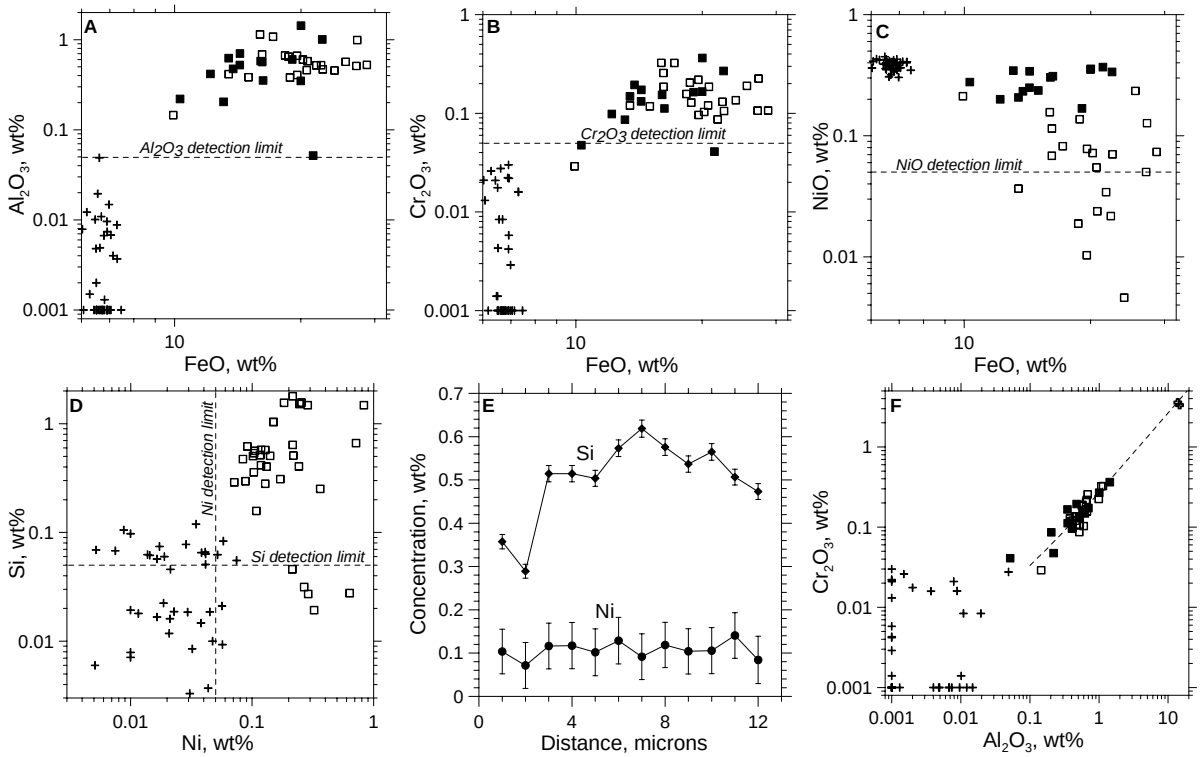

Figure 4. Concentrations of Al_2O_3, Cr_2O_3, FeO and NiO in forsterite, impact melt, and chlorite (A-C, F) and Si and Ni in source metal and metal beads (D,E). A-C: Crosses – forsterite, filled squares – silicate melt without metal beads, open squares – silicate melt with embedded metal beads. D: Crosses – Si, Ni-free source metal, open squares – metal beads embedded in silicate melt E: Diamonds – Si, crcles – Ni, error bars are 2σ. F: Crosses – forsterite, filled squares – silicate melt without metal beads, open squares – silicate melt with embedded metal beads, Swiss crosses – chlorite; the linear least-square fit (R=0.83) of both populations of silicate melts (dashed line) extends to the compositions of Al-rich chlorite, identifying it as the source of Al and Cr in the silicate melts.

Rather high contents of Al_2O_3 and Cr_2O_3 in the silicate melt require a high degree of target homogenization most likely in the plasma cloud and/or ablation melt layer at the target surface by incorporating Al_2O_3 and Cr_2O_3 from the minute grains of Al-rich chlorite (Fig. 4F).

The lack of incipient melting of the targets along with the occurrence of the melt along grain boundaries and cracks in mineral grains point to injection and quenching of melt formed at the target surfaces. We conclude that the metal-silicate melt in our targets represents a portion of the high P-T ablation melt driven into the cold target by the shock wave; the remaining melt along with the shocked and shattered target minerals was lost upon pressure release.

3.3 Interpretation of experimental results: New techniques

The major challenges we faced with in the course of our study were (1) How to capture high P-T laser ablation produced melts, (2) How to calculate pressures and temperatures of those melts, and (3) How to quantify shock-induced mixing both in laser-ablation experiments and during the giant impact phase of planetary formation.

The technique for capturing the laser ablation produced melts came out of our experiments somewhat inadvertently. Our experimental design turned out to be advantageous in two ways: the experimental timescales were too short for an incipient melting inside the target while the high porosity of our targets allowed trapping and quenching of melts produced in the high P-T ablation zone.

To calculate the P and T in our experiments we have developed a mathematical model of the processes involved in the production of the melts trapped in the targets (Remo et al., 2008b). First, we calculated the pressure, P_c, in the plasma region from known values of laser intensity (I), wavelength (λ), average atomic mass (A), and ionization level (Z): $P_c = 1.034 \times 10^{-9} (I/\lambda)^{2/3} (A/(Z+1))^{1/3}$ (GPa). Then the temperature in the plasma region, T_c, is $T_c = 11.4\ (A/(1+Z))^{1/3} (I\lambda^2)^{2/3}$ (KeV),with 1 eV = 11,606 K.

At the interface between the plasma region and the ablation region the relevant hydrodynamic conservation conditions are: $\rho_c\, v_T = \rho_{abl}\, v_{abl}$ (mass conservation) and $P_c + \rho_c\, v_T^2 = P_{abl} + \rho_{abl}\, v_{abl}^2$ (momentum conservation). It is generally assumed (Atzeni & Meyer-ter-Vehn, 2004) that the critical density of the plasma is 10-100× lower than the density of the ablation region underneath it. Accepting a conservative value of 100 ($\rho_c = \rho_{abl}/100$), the boundary condition of $dP \neq 0$ yields: $P_{abl} = P_c + \rho_c\, v_T^2 = 1.5\, P_c$. Then the temperature in the ablation region, T_{abl}, is: $T_{abl} = T_c\, (P_{abl}/P_c)(\rho_c/\rho_{abl})$.

The three ZBL targets were irradiated with the intensities of 2.2 (ZBL-13), 2.8 (ZBL-16), and 5.8 (ZBL-10) TW/cm^2. For these intensities and the laser wavelength of 527 μm the pressures and temperatures at the top of the ablation zone were 228 GPa and 17,823 K for ZBL-13, 276 GPa and 21,121 K for ZBL-16, and 450 GPa and 34,470 K for ZBL-10. The estimated uncertainties of these values are ~10 rel. %, with the uncertainty of the laser intensity being the main contributor. These values are in a very good agreement (Fig. 5) with the similar experiments on laser-induced shock melting of fused silica and quartz reported by (Hicks et al., 2006*)* who measured temperatures of shocked materials by an optical pyrometer.

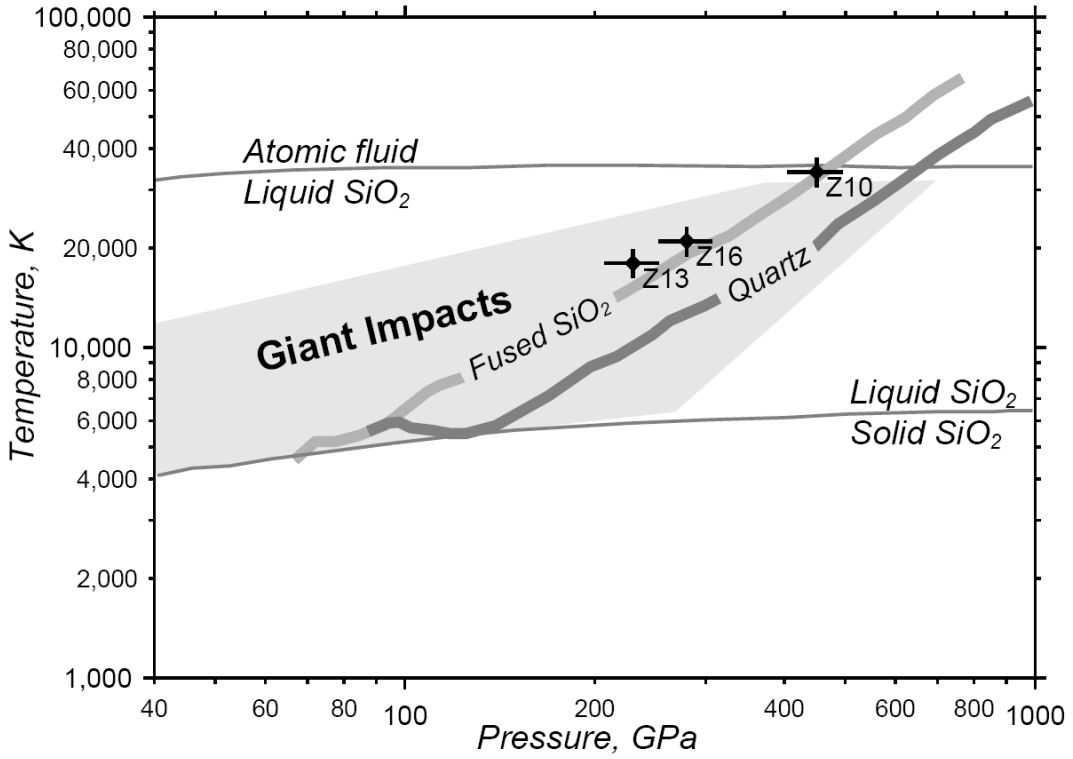

Figure 5. Experimental pressures and temperatures for the ZBL targets are shown by labeled circles with 10% error bars. The Hugoniots for the fused silica and quartz, estimated phase boundaries for solid, liquid and atomic silica fluid, and Giant Impact field are from Hicks et al. (2006).

The problem of scaling of our experimental results to the planetary scale is discussed in sections 3.4 and 3.5.

3.4 Target homogenization timescales: Evidence for the Richtmyer-Meshkov instabilities

The observed homogenization of Cr and Al in the targets studied requires an effective mixing of the target materials on a short timescale, with neither the mixing mechanism nor the exact timescale being known. The timescale is only loosely constrained by a laser pulse width (~0.1 -0.4 nsec) and the shock transit time across the target (~1200 nsec). To get an idea on how such mixing could have occurred, we performed a theoretical analysis of the processes involved in production and evolution of shock-induced melting using the ZBL-16 experiment as an example.

The isothermal speed of sound in the plasma region (U_T) is ~81 km/s (calculated from the laser intensity of I = 2.8 TW/cm^2 = $4\rho_{crit}(U_T)^3$ and the critical density (ρ_{crit} = 1.33x10^{-2} g/cm^3). The compression/shock wave speed in the ablation region is ~0.01U_T to 0.05U_T due to the density difference between the plasma and ablation region. This is relatively consistent with the measured average shock compression wave velocity through the target of 1.91 km/s. In the ablation region the peak shock pressure is estimated (Remo et al 2008a,b) to be ~ 276 GPa at a temperature of ~21,000 K. The shock transit time through the 2.27 mm thick target was 1190 ns. However, the real timescales of high T and P in the target may only have been a factor of about 5

to 10 times the laser pulse time (Swift et al 2004), thus for calculations below we use the maximum value of 10 to obtain the most conservative estimate of timescales.

The ablation rate $dm/dt = \rho_a U_{\text{ablation}}$ where ρ_a is the average target density (~3.4 g/cm^3) and the ablation velocity (U_{ablation}) is ~$0.01 U_T$ to $0.05 U_T$. The ZBL-16 target central crater depth is 470 μm and the estimated ablation depth (d) is 250 μm (Remo et al., 2008). If the entire process was ablative then the total ablation time is in the range of 60 to 310 ns, about 150 to 800 times the laser pulse time. If homogenization was ablation driven, then homogenization of the melt produced in the ablation region would have to have occurred on this timescale or faster. The linear scale of homogenization is the diameter of the crater (~1 mm). Assuming homogenization occurred by diffusion we calculate an effective diffusion coefficient of $D = (L_{\text{diff}}/2)^2/t$ ~0.81 to 4.1 m^2/s from the total time available during ablation (t) and the diffusion length scale (L_{diff}). Independently, the maximum values of diffusion coefficients of Si and Fe in the ablation zone ($T \approx 21{,}000$ K) can be estimated from the thermal conductivity (K) values computed by the MULTI code using the Sesame EoS (Ramis et al. 1988) and extrapolated experimental values (Monaghan & Quested, 2001) which yield a range from 10^{-5} to 5.5×10^{-5} m^2/s. This corresponds to a diffusion length scale in the range 1 to 5 μm – a factor of 200 to 1000 smaller than the observed mixing length scale of ~1 mm). Because our experimental *apparent D* value is at least a factor of ~10^4 higher than likely D values, the efficient mixing observed in our experiments requires a mechanism other than diffusion.

It is known that a high pressure shock wave drives fluids of different densities at different rates, creating turbulent mixing interfaces due to Richtmyer-Meshkov (RM) instabilities. Laser irradiation induces a shock wave propagating through the target and produces RM instabilities in high power laser ablation experiments (Velikovich et al., 2000). It provides the seed for the Rayleigh-Taylor (RT) instability that develops during the acceleration phase of impulse. The RM instability scale (L) for a shock wave driven process in dense (molten) liquids is obtained from the following simple relationship (Atzeni & Meyer-ter-Vehn, 2004): $L = An\tau U_{\text{impulse}}$, where $A = (\rho_1 - \rho_2)/(\rho_1 + \rho_2)$ is the Atwood number (~0.4 for our experiment based on densities of metal and silicate), τ is the laser pulse length (0.39 ns), n is the duration of the shock process in multiples of τ. The impulse velocity (U_{impulse}) that drives turbulent mixing can be calculated from an estimate of the relative amount of ablation (high P, T melting) and the isothermal speed of sound in the plasma (U_T) by the equation (Atzeni & Meyer-ter-Vehn 2004): $U_{\text{impulse}} = -2U_T \ln x$ where $x = m(t)/m_o$ where $m(t)$ is the remaining mass at time t and m_o is the initial mass. Substituting $U_{impulse}$ yields $L = -2An\tau U_T \ln x$. Here $n \approx 10$ for the RM because it demands a shock process that will not persist much longer than the high pressure plasma pulse. While $x = m(t)/m_o$ for our experiment cannot be precisely determined, it is estimated to be ~0.10 (>90% ablation and <10 % injected into the target) which yields a value of $L \sim 582$ μm for the ZBL-16 experiment ($U_T = 81$ km/s)). This is very similar to the required equilibration length scale of ~0.5 mm (radius of crater) and much larger than the estimated diffusion length scale (~1 to 5 μm). Thus, we conclude that the observed Cr and Al mixing in the silicate melt is consistent with being produced by the RM instability caused by the impulse shock. The assumption here is that the process that drives the metal-silicate mixing in our experiment also homogenizes Cr and Al from the chlorite grains in the target material.

The turbulent mixing induced by RM in our experiments has important implications to mixing during the final stages of Earth's accretion. What is required here is that the collision of Earth and an impactor propagates a shock wave over a broad volume for a significant period of time. In this case the impulse velocity for the planet collision can be calculated from the speed of

the impactor ($U_{Impactor}$) in a similar way to our single pulse laser ablation experiment. The energy density of a giant impact modeled by Canup (2004) with $U_{Impactor} \approx 10$ km/s is similar to that of the ZBL-16 shot producing the ~276 GPa pressure in the laser target ablation zone. The RM length scale for the planet collision is: $L_{Planet} = -2A_{Planet}\tau_{Planet}U_{Impactor}\ln x_{Planet}$ (x_{Planet} is the mass fraction of melt produced at the initial impact that is not ablated). It depends on the amount of melting occurring in the collision process. Because the turbulent mixing is linearly dependent on τ, there is a simple scaling of our experimental results to the planetary bodies involved in the formation of the Earth-Moon system: $\tau_{\mathrm{Planet}} = (U_{\mathrm{T}}/U_{\mathrm{Impactor}})(\ln x_{laser}/\ln x_{\mathrm{Planet}})(L_{\mathrm{Planet}}/L_{\mathrm{laser}})n_{\mathrm{laser}}\tau_{\mathrm{laser}}$ assuming similar Atwood numbers for the laser target and the planet. We use A_{Planet} ~0.4 and a conservative value for the amount of the melt produced in the impact zone that is initially ejected from the Earth ($x_{\mathrm{Planet}} = 0.5$), based on the simulation by Canup (2004). Thus, the RM mixing length-scales is 2200, 6400 and 17000 km for times of 0.11, 0.32 and 0.86 hours, respectively. These results are compared in Figure 6 with cartoons of three early stages of the simulation of the Earth-Moon forming impact process modeled by Canup (2004). Thus, if this collision can maintain the high *P,T* at the interface, the shock wave induced turbulence will effectively mix the interior of the impactor in less than 1 hour. We note that the reverberation shock experiments (Tschauner et al. 2005) also imply that RM instabilities during a giant impact would lead to an effective mixing of the impactor's core. Thus, the RM instabilities caused by the shock conditions during the giant impact can result in efficient homogenization of impactor core and terrestrial mantle material.

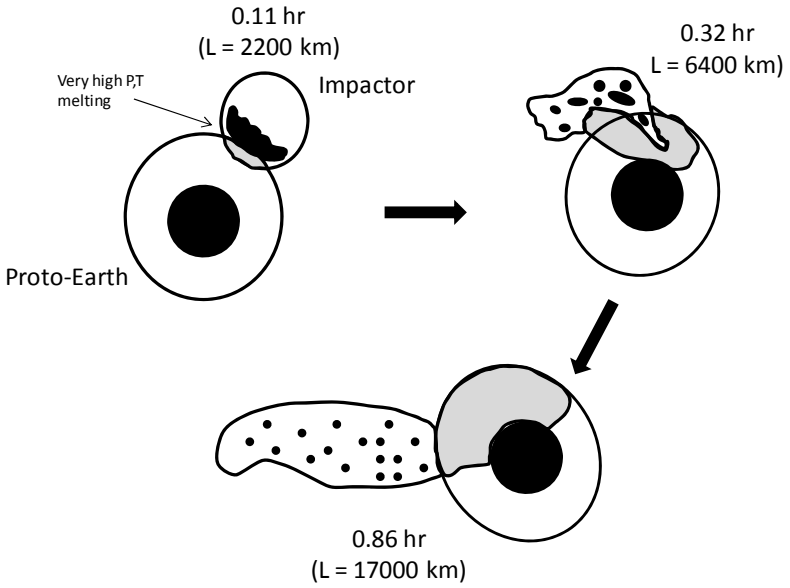

Figure 6. Cartoon based on the SPH simulations of the Moon-forming giant impact by Canup (2004). An initial oblique impact initiates RM instabilities in both objects. The shaded area denotes very high P, T melt.

3.5 Metal-silicate equilibration: Implications for the Hf-W dating of core formation

The generally small size of metal droplets enclosed in the shock-produced silicate melt is consistent with estimated diffusion lengths of Fe and Si in the ablation zone (section 3.4), suggesting that the metal-silicate equilibration was most likely a diffusion-driven process. Then

using the estimated D value of 3×10^{-5} m^2/sec we can scale our experiments to the conditions of the giant impact (Fig. 7). It takes only a minute to extract Ni into a 10 cm metal droplet from the silicate melt surrounding it.

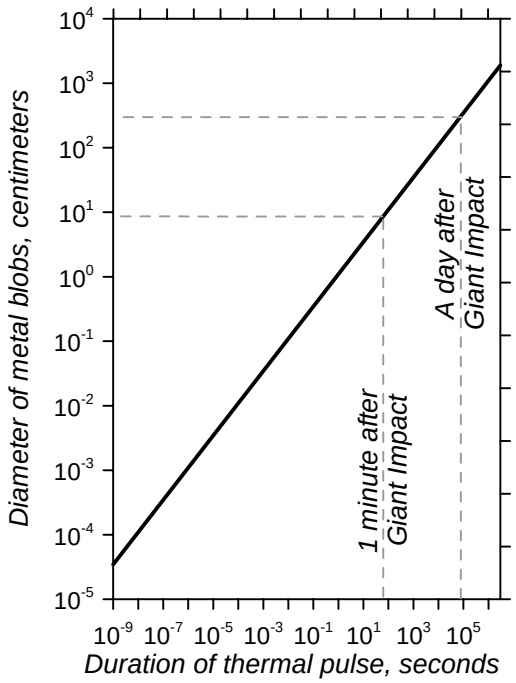

Figure 7. Timescales for Ni equilibration between silicate melt and metal droplets.

The experiments also suggest that the post-giant impact terrestrial magma ocean could have been much more ferrous (15-25 wt.% FeO) than the current mantle (7.6 wt.%). This implies that more than half of FeO from the primary magma ocean must have been reduced to Fe to be transported into the Earth's core as metal droplets. The high efficiency of this process in metal-silicate equilibration has already been demonstrated (Rubie et al. 2003; Melosh & Rubie 2007). It is driven by Rayleigh-Taylor (RT) instabilities causing further mixing of metal and silicate during the rainout of metal into the core following the giant impact. Thus, the metal-silicate mixing was started by RM and followed by RT mixing. The RT instabilities reduce the length-scale of metal blobs (km-sized) in the magma ocean to ~1 cm leading to rapid chemical and isotopic equilibration (Rubie et al. 2003). Therefore, our new experimental results provide strong support for ^{182}Hf-^{182}W dating of core-mantle differentiation by using the standard global magma ocean model that yields a mean time of core formation (64% of the mass) of 11 Myr (Yin et al. 2002). If this model is modified to include a Mars-sized impactor at the end of accretion, then the Earth-Moon system forms ~32 Myr after Solar System formation (Jacobsen 2005).

4. Publications resulting from the award:

Hammerling P. & Remo J. L. (2006) Pulsed femtosecond laser-target momentum coupling in the high-intensity regime, *High-Power Laser Ablation VI. (C. R. Phipps, ed.). Proc. SPIE*, **6261**, 2L.

Petaev M. I., Jacobsen S. B., Remo J. L., Adams R. G. & Sasselov D. D. (2006) Laser Simulation of High P-T Planetary Processes, *American Geophysical Union*, Fall Meeting 2006, abstract #MR53D-05.

Remo J. L., Adams R. G., Petaev M. I., Jacobsen S. B. & Sasselov D. D. (2006) Experimental Study of High-Energy Processing of Protoplanetary Materials, *American Geophysical Union*, Fall Meeting 2006, abstract #MR51B-0967.

Petaev M. I., Jacobsen S. B., Remo J. L., Adams R. G. & Sasselov D. D. (2007) Experimental study of high-energy processing of protoplanetary materials. *Lunar Planet. Sci. Conf*. **38**, #1822.

Remo J. L., Adams R. G., Petaev M. I., Jacobsen S. B. & Sasselov D. D. (2007) Laser simulation of high P-T planetary processes. *Lunar Planet. Sci. Conf*. **38**, #1847.

Remo J. L. (2007) Classifying solid planetary bodies. In: Astrodynamics, Space Missions, and Chaos III, (Trends in Astrodynamics and Applications), *E. Belbruno and P. Gurfil, ed.*, *AIP conf. proc.* **886***,* 284-299.

Remo J. L., Adams R.G. & Jones M. C. (2007) Atmospheric electromagnetic pulse propagation effects from thick targets in terawatt laser target chamber, *Applied Optics*, **46**, 6166- 6175.

Petaev, M. I., Jacobsen, S. B., Remo, J. L., Adams, R. G. & Sasselov, D. D. (2008) Experimental study of high-energy processing of protoplanetary materials: implications for the post giant impact Earth. *Lunar Planet. Sci. Conf*. **39**, #1391.

Remo J. L., Petaev M. I. & Jacobsen S. B. (2008) Experimental simulation of high P-T planetary processes: physics of laser-induced shocks in solid and powdered targets. *Lunar Planet. Sci. Conf*. **39**, #1420.

Jacobsen S.B., Remo J.L., Petaev M.I. & Sasselov D.D. (2008) Hf-W equilibration in a magma ocean at very high P and T. *Geochim. Cosmochim. Acta*, **72**, Supplement 1, A419.

Jacobsen S. B., Ranen M. C., Petaev M. I., Remo J. L., O'Connell R. J. & Sasselov D. D. (2008) Isotopes as clues to the origin and earliest differentiation history of the Earth. *Phil. Trans. R. Soc. A*, **366**, 4129–4162.

Remo J. L. and Furnish M. D. (2008) Analysis of Z-pinch shock wave experiments in meteorite and planetary materials, *Intl. J. Impact Eng.*, **35**, 1516-1521.

Remo J. L. (2008) Plasma radiation hydrodynamics and momentum coupling, *High-power laser ablation VII (ed. C. R. Phipps), Proc. SPIE,* **7005**, 2J1-2J9.

Remo J. L. and Adams R. G. (2008) High energy density laser interaction with planetary and astrophysical materials: methodology and data. *High-power laser ablation VII (ed. C. R. Phipps), Proc. SPIE,* **7005**, 2M1–2M10.

Remo J. L., Jacobsen S. B., Petaev M. I., Adams R. G. & Sasselov D.D. (2008) Laser shock melting of a metal-silicate target and the timing of the giant Moon-forming impact on Earth. *Nature*, under revision.

Jacobsen S.B., Remo J.L., Petaev M.I. & Sasselov D.D. (2009) Hf-W chronometry and the timing of the giant Moon-forming impact on Earth. *Lunar Planet. Sci. Conf*. **40**, #2054

Jacobsen S.B., Remo J.L., Petaev M.I. & Sasselov D.D. (2008) The first law of cosmochemistry. *Geochim. Cosmochim. Acta*, in press.

Petaev Jacobsen S. B., Remo J. L., Adams R. G. & Sasselov D. D. (2009) Experimental study of high-energy processing of protoplanetary materials: implications for the post giant impact

Earth. *Earth Planet. Sci. Lett*. (in prep).

Remo J. L. & Furnish M. D. (2009) Soft X-ray shock loading and momentum coupling in meteorite and planetary material. *Phys. Rev*. (in prep).

5. References:

Atzeni S. & Meyer-ter-Vehn J. (2004) The physics of inertial fusion, Oxford Univ. Press, Oxford.

Canup R. M. (2004) Simulations of a late lunar-forming impact. *Icarus* **168**, 433-456.

Hicks D. G., Boehly T. R., Eggert J. H., Miller J. E., Celliers P. M. & Collins G. W. (2006) Dissociation of liquid silica at high pressures and temperatures. *Phys. Rev. Lett.* **97**, 025502-025506.

Jacobsen S. B. (2005) The Hf-W isotopic system and the origin of the Earth and Moon. *Ann. Rev. Earth Planet. Sci.* **33**, 531-570.

Melosh H. J. & Rubie D. C. (2007) Ni Partitioning in the Terrestrial Magma Ocean: A Polybaric Numerical Model. *Lunar and Planetary Science* **38**, #1593.

Ramis R., Schmalz R. & Meyer-ter-Vehn J. (1988) MULTI – A computer code for one-dimensional multi-group radiation hydrodynamics. *Computer Physics Communications*, **49**, 475-505.

Remo J. L., Jacobsen S. B., Petaev M. I., Adams R. G. & Sasselov D.D. (2008a) Laser shock melting of a metal-silicate target and the timing of the giant Moon-forming impact on Earth, *Nature*, submitted.

Remo J. L., Petaev M. I. & Jacobsen S. B. (2008b) Experimental simulation of high P-T planetary processes: physics of laser-induced shocks in solid and powdered targets. *Lunar Planet. Sci.* **39**, # 1420.

Rubie D. C., Melosh H. J., Reid J. E., Liebske C. & Righter K. (2003) Mechanisms of metal-silicate equilibration in the terrestrial magma ocean. *Earth Planet. Sci. Lett.* **205**, 239-255.

Swift D. C., Tierney T. E. IV, Kopp R. A. & Gammel J. T. (2004) Shock pressures induced in condensed matter by laser ablation. *Physical Review E* **69**, 036406-1-9.

Tschauner O., Willis M. J., Asimow P. D. & Ahrens T. J. (2005) Effective liquid metal-silicate mixing upon shock by power-law droplet size scaling in Richtmyer-Meshkov like perturbations. *Lunar Planet. Sci.* **36**, # 1802.

Velikovich A. L., Dahlburg J. P., Schmitt A. J., Gardner J. H., Phillips L., Cochrana F. L., Chong Y. K., Dimonte G. & Metzler N. (2000) Richtmyer–Meshkov-like instabilities and early-time perturbation growth in laser targets and Z-pinch loads, *Physics of Plasmas*, **7**, 1662-1671.

Yin Q.-Z., Jacobsen S. B., Yamashita K., Blichert-Toft J., Telouk P. & Albarede F. (2002) A short timescale for terrestrial planet formation from Hf-W chronometry of meteorites. *Nature* **418**, 949-952.